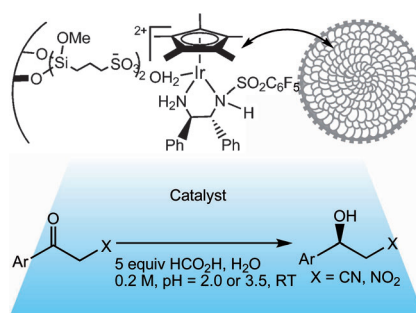


## COMMUNICATIONS


**Pores that put your reaction in a spin!**

A recoverable mesoporous silica exhibits excellent catalytic activity and enhanced enantioselectivity for the reduction of  $\alpha$ -cyano and  $\alpha$ -cyanoacetophenones that ascribes the synergistic effect of its phase-transfer functionalized cetyltrimethylammonium bromide and confined chiral organoiridium catalytic nature.



B. Deng, T. Cheng,\* M. Wu, J. Wang,  
G. Liu\*

■ ■ - ■ ■

**Enantioselective Reduction of  $\alpha$ -Cyano  
and  $\alpha$ -Nitro Substituted  
Acetophenones Promoted by  
a Bifunctional Mesoporous Silica** 

DOI: 10.1002/cctc.201300340

# Enantioselective Reduction of $\alpha$ -Cyano and $\alpha$ -Nitro Substituted Acetophenones Promoted by a Bifunctional Mesoporous Silica

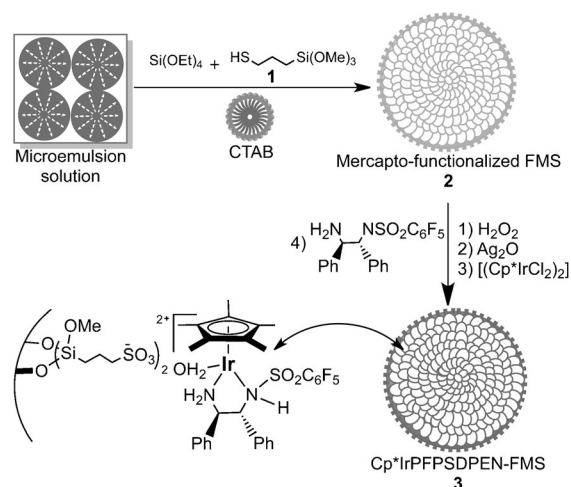
Boxin Deng, Tanyu Cheng,\* Meng Wu, Jinyu Wang, and Guohua Liu\*<sup>[a]</sup>

Exploration of silica-based mesoporous supports to immobilize chiral organometallic complexes for asymmetric catalysis has attracted a great deal of interest, owing to their relatively large surface area/pore volume and tunable pore dimension/well-defined pore arrangement.<sup>[1]</sup> These salient features are not only beneficial to the dispersibility of active species to promote the catalytic performance, but also can adjust the chiral microenvironment of the active centers to enhance enantioselective performance. Recently, many successful examples, such as the mesoporous SBA series<sup>[2]</sup> and the MCM series<sup>[3]</sup> of materials as supports, have been applied to anchor various organometallic complexes, and some heterogeneous catalysts have presented excellent catalytic activity in asymmetric reactions. Most of these heterogeneous catalysts, however, do only exhibit comparable catalytic activities and/or enantioselectivities relative to their homogeneous counterparts. Therefore, how can we develop new silica-based mesoporous materials as supports and take advantage of this special functionalized material to promote catalytic performance?

Flowerlike mesoporous silica (FMS) as a type of novel mesoporous material<sup>[4]</sup> shows potential advantages that have not been explored in asymmetric catalysis as yet. Besides easy preparation and functionalization, FMS-based supports possess relatively short mesochannels and special silicate cavum. This unique mesoporous morphology has a potential confinement effect to enhance its enantioselectivity.<sup>[5]</sup> Because self-assembly of this kind of materials often requires cetyltrimethylammonium bromide (CTAB) as a structure-directing template reagent, the residual CTAB molecules within its silicate network can improve the phase-transfer catalytic properties of the material, which can facilitate asymmetric reactions in an aqueous medium, and also improve the catalytic activity. Taken together, it is reasonable to expect that self-assembly of chiral organometallic-functionality within a functionalized FMS silicate network could possess high catalytic activity and enantioselectivity in an aqueous asymmetric catalysis system.

As an effort to develop highly efficient heterogeneous catalysts,<sup>[6]</sup> in this contribution, we directly bond an organoiridium complex within mesoporous material followed by complexation with a chiral ligand, and develop one chiral functionalized mesoporous material, consisting of CTAB functionality as a phase transfer catalyst and chiral organoiridium functionality as a chiral promoter. As expected, CTAB functionality can greatly enhance the catalytic performance, while the enantioselectivity can be further improved as a result of the synergistic effect. Furthermore, the heterogeneous catalyst can be readily recycled and reused at least 10 times without reducing its catalytic activity.

The chiral Cp\*IrPFSPDEN-functionalized FMS material (Cp\*IrPFSPDEN:<sup>[7]</sup> Cp\* = pentamethyl cyclopentadiene, PFSPDEN = (*S,S*)-pentafluorophenylsulfonyl-1,2-diphenylethylenediamine), abbreviated as Cp\*IrPFSPDEN-FMS (**3**), was prepared as outlined in Scheme 1. Firstly, the microemulsion solu-



Scheme 1. Preparation of the heterogeneous catalyst **3**.

tion formed in mixture solvents of  $\text{NH}_3\text{-H}_2\text{O}$ , ethyl ether and tetraethoxysilane (TEOS) was assembled using CTAB as a structure-directing template, which was continuously grown among TEOS and 3-mercaptopropyltrimethoxysilane (**1**) to give Mercapto-functionalized FMS (**2**) in formation of a white powder. The oxidation<sup>[8]</sup> of **2** using  $\text{H}_2\text{O}_2$  as the oxidant followed by the continuous ion exchange with  $\text{Ag}_2\text{O}$ <sup>[9]</sup> and  $[(\text{Cp}^*\text{IrCl}_2)_2]$  did then bond successfully the cationic iridium complex within its FMS silicate network. Finally, direct complexation with pentafluorophenylsulfonyl-1,2-diphenylethylenediamine<sup>[10]</sup> afforded the

[a] B. Deng, T. Cheng, M. Wu, J. Wang, Prof. G. Liu  
Key Laboratory of Resource Chemistry of Ministry of Education  
Shanghai Key Laboratory of Rare Earth Functional Materials  
Shanghai Normal University  
No.100 Guilin Rd., Shanghai (P.R. China)  
Fax: (+86)2164321819  
E-mail: tycheng@shnu.edu.cn  
ghliu@shnu.edu.cn

Supporting information for this article is available on the WWW under <http://dx.doi.org/10.1002/cctc.201300340>.

catalyst **3** in formation of light yellow powders (Figures S1–7 in the Supporting Information). The thermal gravimetric (TG/DTA) analysis disclosed that about 7.0% of Cp\*IrPFPSDPEN functionality and 8.8% of the residual CTAB<sup>[11]</sup> were anchored within its FMS silicate network (Figure 1 a, also see in Figure S4 in the SI),

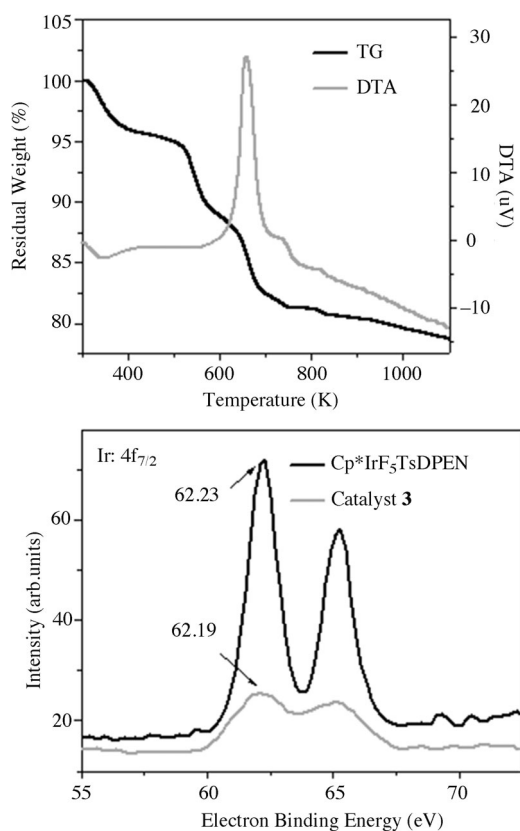


**Figure 1.** a) TG/DTA curves of **3**, b) XPS spectra of Cp\*IrPFPSDPEN and **3**.

in which the mole amount of Cp\*IrPFPSDPEN functionality (0.078 mmol) was nearly consistent with 0.077 mmol (14.80 mg) of Ir loading per gram catalyst detected by inductively coupled plasma (ICP) optical emission spectrometer analysis.

The incorporation of Cp\*IrPFPSDPEN functionality within its silicate network is confirmed by the solid-state <sup>13</sup>C CP/MAS NMR spectrum (Figure S2 in the SI), in which the catalyst **3** presented clearly the characteristic peaks of C<sub>5</sub>Me<sub>5</sub> moieties around  $\delta = 87$  ppm corresponding to the C atoms of Cp\* ring and around  $\delta = 10$  ppm for the C atoms of methyl groups in Cp\* ring. These observations were strongly related to those of the homogeneous counterpart, Cp\*IrPFPSDPEN,<sup>[7a]</sup> which suggested that the catalyst **3** had the same well-defined single-site active center. In particular, the carbon signals for the residual CTAB functionality could be observed clearly. The peaks around  $\delta = 11$  and 28 ppm were ascribed to the C of methyl (or methylene) groups without connection to nitrogen atom in CTAB molecule and the peaks around  $\delta = 59$  ppm overlapped partly by nonhydrolyzed methoxide groups (CH<sub>3</sub>O)<sup>−</sup><sup>[12]</sup> were belonged to the C atoms of methyl (or methylene) groups connected to nitrogen atom in CTAB molecule as marked in its <sup>13</sup>C

CP/MAS NMR spectrum. These observed peaks demonstrated that the residual CTAB molecule remained in its silicate network proved by thermal gravimetric (TG/DTA) analysis.

The <sup>29</sup>Si CP/MAS NMR spectrum (Figure S3 in the SI) revealed that the catalyst **3** possessed the inorganosilicate framework of (HO)Si(OSi)<sub>3</sub> with organosilicate RSi(OSi)<sub>3</sub> (R = Cp\*IrPFPSDPEN functionality) as the part of silica wall,<sup>[13]</sup> in which the strongest Q<sup>3</sup> peak that originated from inorganosilicate species confirmed its framework of (HO)Si(OSi)<sub>3</sub>, while the strongest T<sup>3</sup> peak that derived from organosilicate species proved its organosilicate wall of RSi(OSi)<sub>3</sub>. Furthermore, the nitrogen adsorption–desorption isotherm disclosed that the catalyst **3** was mesoporous and was very comparable to those reported in the literature.<sup>[14]</sup> The additional large N<sub>2</sub> uptakes and H3 hysteresis at the relative pressure near 1.0 have been previously described as a large amount of macropores with a slit shapes (Figure S6).<sup>[14a]</sup>

The scanning electron microscopy (SEM) and transmission electron microscopy (TEM) images demonstrated that the catalyst **3** was composed of aggregates of particles with average diameter around 1.4  $\mu$ m (Figure 2 a–b). In particular, the TEM image with a chemical mapping technique indicated that the iridium active centers were uniformly distributive within its silicate network (Figure 2 c). Based on the above characterizations and analyses, a safely conclude could be drawn, in which chiral organoiridium-functionalized mesoporous silica with inorganosilicate network of (HO)Si(OSi)<sub>3</sub>, the well-defined single-site Cp\*IrPFPSDPEN active center, controllable CTAB functionality

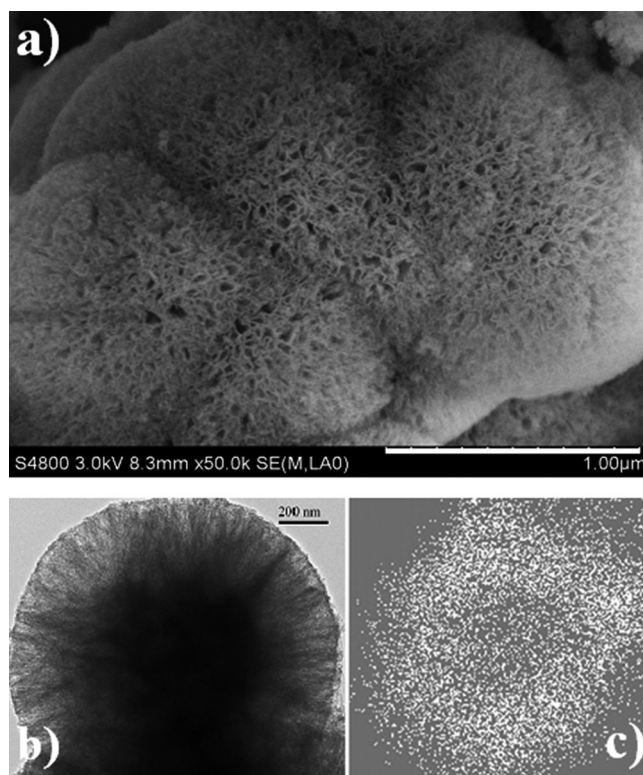


**Figure 2.** The a) SEM, b) TEM images of the catalyst **3** and c) TEM with a chemical map of **3** and the distribution of Si (white) and Ir (grey). Scale bars: a) 1  $\mu$ m, b,c) 200 nm.

and the uniformly distributed iridium active centers within its silicate network could be readily constructed in this case.

Summarized in Table 1 is the asymmetric transfer hydrogenation of a range of  $\alpha$ -cyanoacetophenones in an aqueous medium, in which  $\text{HCO}_2\text{H}$  worked as a hydrogen source and 0.25% mol of this silica material acted as a catalyst according

**Table 1.** **3**-catalyzed asymmetric transfer hydrogenation of  $\alpha$ -cyano and  $\alpha$ -cyano acetophenones.<sup>[a]</sup>

Entry	Ar	X	Conv. [%] <sup>[b]</sup>	ee [%] <sup>[b]</sup>
1	Ph	CN	> 99	97(94) <sup>[c]</sup>
2	Ph	CN	91	95 <sup>[d]</sup>
3	Ph	CN	> 99	93 <sup>[e]</sup>
4	Ph	CN	87	93 <sup>[f]</sup>
5	4-FPh	CN	> 99	96
6	3-ClPh	CN	> 99	94
7	4-MePh	CN	> 99	95
8	3-MeOPh	CN	> 99	97
9	2-furyl	CN	> 99	99
10	2-thiophenyl	CN	> 99	95
11	Ph	$\text{NO}_2$	> 99	97
12	4-FPh	$\text{NO}_2$	> 99	95
13	4-ClPh	$\text{NO}_2$	> 99	94
14	2-ClPh	$\text{NO}_2$	> 99	91
15	4-MePh	$\text{NO}_2$	> 99	96
16	4-MeOPh	$\text{NO}_2$	> 99	95

[a] Reaction conditions: the catalyst **3** (26.1 mg, 2.0  $\mu\text{mol}$  of Ir based on the ICP analysis),  $\alpha$ -cyanoacetophenones ( $\alpha$ -nitroacetophenones) (0.80 mmol) and the aqueous solution of formic acid (5.0 equiv, 1.0 M formate solution, 0.2 M overall concentration, for X = CN, pH 3.5; for X =  $\text{NO}_2$ , pH 2.0), at room temperature for 10–20 h. [b] Determined by chiral HPLC analysis (Figure S8 in the SI). [c] Data in the bracket were obtained using the homogenous  $\text{Cp}^*\text{IrPFPPSDPEN}$  as a catalyst reported in the literature.<sup>[7a]</sup> [d] Data were obtained using the catalyst **3** with S/C = 600. [e] Data were obtained using CTAB plus its homogeneous  $\text{Cp}^*\text{IrPFPPSDPEN}$  as a catalyst. [f] Data were obtained using the pure FMS plus  $\text{Cp}^*\text{IrPFPPSDPEN}$  as a heterogeneous catalyst.

to the reported methods.<sup>[7a]</sup> In general, excellent conversions, no by-products, and high enantioselectivities were obtained for all tested substrates. Taking benzoylacetone nitrile as an example, the catalyst **3** gave (*S*)-3-Hydroxy-3-phenylpropanenitrile with more than 99% conversion and 97% enantiomeric excess (*ee*), for which the *ee* value was higher than that of its homogeneous  $\text{Cp}^*\text{IrPFPPSDPEN}$  (entry 1 versus entry 1 in bracket). Of particular note was that the asymmetric reaction could be run at a much higher ratio of substrate-to-catalyst without greatly affecting its *ee* value, as exemplified by the asymmetric transfer hydrogenation of benzoylacetone nitrile at S/C = 600 (entry 2). Moreover, it was also found that the electronic properties of substituents at acetophenone did not affect significantly their enantioselectivities as its homogeneous behavior, in which the asymmetric reactions with electron-rich and electron-poor substituents at  $\alpha$ -cyanoacetophenones were equally efficient (entries 5–10).

The asymmetric reactions could be completed within 10 h in most cases, which were dramatically shorter than the 24 h re-

quired by the homogeneous counterpart under the similar conditions. Interestingly, the catalyst **3** presented the enhanced enantioselectivity relative to its homogenous counterpart for all tested substrates.<sup>[7a]</sup> Both behaviors strongly suggest that the bifunctional feature of the heterogeneous catalyst **3**, which contains the CTAB functionality as a phase transfer catalyst, increased greatly its catalytic performance in this aqueous catalytic system, while the enantioselectivity could be enhanced by the synergistic effects<sup>[6a–d]</sup> of a unique phase-transfer function and the confined chiral organoiridium catalyst.

To gain better insight into the nature of the synergistic effect, two parallel experiments were investigated using pure small molecule (CTAB) plus its homogeneous  $\text{Cp}^*\text{IrPFPPSDPEN}$  (Table 1, entry 3) and the pure FMS material plus its homogeneous  $\text{Cp}^*\text{IrPFPPSDPEN}$  (Table 1, entry 4) as catalysts when the asymmetric transfer hydrogenation of benzoylacetone nitrile was chosen as probe reaction. It was found that the asymmetric reaction given in entry 3 could be completed in 10 h with 93% *ee*, whereas entry 4 gave the corresponding alcohol with 87% conversion and 93% *ee* in 10 h. In the case of entry 3, if the same reaction time as catalyst **3** was used, a similar phase-transfer function by the CTAB molecule also promotes the catalytic performance, although a lower *ee* value is now given, which suggests that the asymmetric reaction only retained its original homogenous enantioselectivity.<sup>[7a]</sup> This fact disclosed that the enhanced *ee* value given for catalyst **3** was derived from the nature of the catalyst material itself. In the case of entry 4, the lower conversion than catalyst **3** indicated that the main part of the homogeneous catalyst derived from non-covalent adsorption within its silicate network did participate in the catalytic process, while the small part of the homogeneous catalyst derived from non-covalent adsorption did not work during the catalytic process, owing to blockage or disorder. As a result, the catalyst in the entry 4 had a lower conversion than heterogeneous catalyst **3**. In addition, the lower *ee* value given in entry 4 further confirms the enantioselective nature of the homogeneous chiral catalyst. More importantly, when the catalyst of entry 4 was treated by Soxhlet extraction, the reused catalyst gave only tiny products. This fact demonstrated that the disturbance coming from the homogeneous catalyst by means of noncovalent physical adsorption had been eliminated. All these observations consolidated that the unique phase-transfer functionalized cetyltrimethylammonium bromide and confined chiral organoiridium catalytic nature as a result of the synergistic effect in the heterogeneous catalyst **3** are responsible for its excellent conversion and enhanced enantioselectivity. X-ray photoelectron spectroscopy (XPS) investigations (Figure 1b) further supported our conclusions. It was found the catalysts **3** had the nearly same Ir  $4f_{7/2}$  electron binding energy as the parent counterpart (62.19 versus 62.23 eV), further demonstrating that the enhanced enantioselectivity ascribed the synergistic effect of this mesoporous silica rather than the unchanged chiral microenvironment of active center.

In addition to  $\alpha$ -cyanoacetophenones, the heterogeneous catalyst **3** could also be applied to the asymmetric transfer hydrogenation of  $\alpha$ -nitroacetophenones in aqueous medium (en-

tries 11–16). Again, short reaction times, excellent conversions, and enhanced enantioselectivities were obtained all cases. These results demonstrate that catalyst **3** can serve as a general catalyst in the asymmetric transfer hydrogenation of different substrates.

An important feature for design of any heterogeneous catalyst is easy to separate via simple centrifuge and the recovered catalyst can retain its catalytic activity and enantioselectivity after multiple cycles. Remarkably, the catalyst **3** was recovered easily and reused repeatedly when benzoylacetonitrile was chosen as a substrate. In ten consecutive reactions, the reused catalyst **3** still afforded 99% conversion and 94% *ee* (Figure 3,

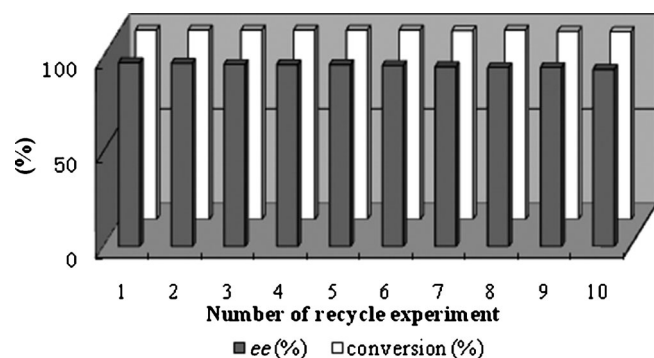


Figure 3. Reusability of **3** using benzoylacetonitrile as a substrate.

Table S1, and Figure S9 in the SI). The high recyclability can be attributed to the unique mesoporous morphology, which significantly decreases the leaching of Ir. An evidence to support the view came from the ICP analysis, in which the amount of Ir after tenth recycle was 13.89 mg per gram catalyst and only 6.1% of Ir was lost.

In conclusion, we have developed a new strategy for the immobilization of chiral organoiridium complexes onto the mesoporous silica, which displays higher catalytic activity and enantioselectivity than its homogeneous counterpart for the asymmetric transfer hydrogenation of  $\alpha$ -cyano and  $\alpha$ -cyanoacetophenones in aqueous medium. More importantly, cetyltrimethylammonium bromide acted as a phase transfer catalyst within its mesoporous silicate network can increase greatly catalytic performance, while the unique mesostructure of mesoporous silica can boost the enantioselectivity. Furthermore, the heterogeneous catalyst can be recovered conveniently and subsequently reused at least 10 times without affecting its catalytic activity. More importantly, this strategy described here might expand to other chiral complexes for asymmetric organic transformations, which represents our future effort.

## Experimental Section

### Preparation of Cp\*IrPFSPDEN-functionalized FMS (**3**)

To a suspension of Mercapto-functionalized FMS (**2**) (1.00 g) in 10.0 mL acetic acid was added a solution of 30% H<sub>2</sub>O<sub>2</sub> (20.0 mL) at room temperature and the resulting mixture was stirred at 100 °C

for 6 h. After cooling down to ambient temperature, the mixture was filtered through filter paper and rinsed with excess ethanol and CH<sub>2</sub>Cl<sub>2</sub>. The collected white solids were suspended in 20.0 mL distilled water again and Ag<sub>2</sub>O (229.0 mg, 1.0 mmol) was added at ambient temperature. The resulting mixture was heated at 90 °C for 6 h. After cooling down to ambient temperature, a solution of 2.0 NH<sub>2</sub>SO<sub>4</sub> (10 mL) was added and stirred overnight. The solids were collected by centrifugation, washing repeatedly with excess distilled water. The collected light grey solids were suspended in the mixture solution (10.0 mL of methanol and 10.0 mL distilled water) again and 199.0 mg (0.25 mmol) of [(Cp\*IrCl<sub>2</sub>)<sub>2</sub>] was added at ambient temperature. The resulting mixture was stirred for 12 h. Finally, 221.0 mg (0.50 mmol) of (*S,S*)-pentafluorophenylsulfonyl-1,2-diphenylethylenediamine was added and the reaction was further stirred for another 6 h at ambient temperature. The mixture was then filtered through filter paper and rinsed with excess water and CH<sub>2</sub>Cl<sub>2</sub>. After Soxhlet extraction in CH<sub>2</sub>Cl<sub>2</sub> solvent to remove homogeneous and unreacted starting materials for 24 h, the solid was dried at ambient temperature under vacuum overnight to afford the catalyst **3** (1.35 g) as a light yellow powder. ICP analysis showed that the Ir loading-amount was 14.80 mg (0.0778 mmol) per gram catalyst. IR (KBr):  $\tilde{\nu}$  = 3416.2 (s), 2928.4 (w), 2857.6 (w), 1630.1 (m), 1496.5 (w), 1457.9 (w), 1082.0 (s), 947.6 (m), 801.8 (m), 699.4 (w), 568.1 (w), 462.2 cm<sup>-1</sup> (m); <sup>29</sup>Si MAS/NMR (79.4 MHz):  $\delta$  = -67.2 (T<sup>3</sup>), -91.3 (Q<sup>2</sup>), -101.5 (Q<sup>3</sup>), -110.4 ppm (Q<sup>4</sup>); <sup>13</sup>C CP/MAS (100.5 MHz):  $\delta$  = 10.1 (CpCH<sub>3</sub>, SiCH<sub>2</sub> and CH<sub>3</sub> of CTAB), 17.7 (SiCH<sub>2</sub>CH<sub>2</sub>), 27.1 (CH<sub>2</sub> of CTAB), 53.1 (CH<sub>2</sub>SO<sub>3</sub>), 59.2, 63.7 (NCH<sub>2</sub> or NCH<sub>3</sub> of CTAB), 70.2, (NCH), 86.6 (C<sub>5</sub> of Cp), 128.0, 130.4, 139.2 ppm (C of Ph); S<sub>BET</sub>: 229.4 m<sup>2</sup>g<sup>-1</sup>, d<sub>por</sub>: 3.60 nm, V<sub>por</sub>: 0.62 cm<sup>3</sup>g<sup>-1</sup>; Elemental analysis (%): C 8.59, H 1.97, N 0.69, S 0.49.

### Catalytic experiments

A typical procedure was as follows: The catalyst **3** (26.1 mg, 2.0  $\mu$ mol of Ir based on the ICP analysis), benzoylacetonitrile (116.0 mg, 0.80 mmol) and the aqueous solution of formic acid (5.0 equiv 1.0 M formate solution, 0.2 M overall concentration, for X = CN, pH 3.5; for X = NO<sub>2</sub>, pH 2.0.) were added in a 10.0 mL round-bottom flask in turn. The mixture was then stirred at room temperature for 10–20 h. During that time, the reaction was monitored constantly by TLC. After completion of the reaction, the catalyst was separated via centrifuge (10000 rmin<sup>-1</sup>) for the recycle experiment. The aqueous solution was extracted by ethyl ether (3  $\times$  3.0 mL). The combined ethyl ether was washed with brine twice and dehydrated with Na<sub>2</sub>SO<sub>4</sub>. After the evaporation of ethyl ether, the residue was purified by silica gel flash column chromatography to afford the desired product. The conversion was calculated by the external standard method and the *ee* value could be determined by a HPLC analysis with a UV-Vis detector using a Daicel OJ-H chiralcel column ( $\Phi$  0.46  $\times$  25 cm).

### Acknowledgements

We are grateful to the China National Natural Science Foundation (20673072), Shanghai Sciences and Technologies Development Fund (10J1400103, 10JC1412300 and 12nm0500500), CSIRT (IRT1269), and Shanghai Municipal Education Commission (12ZZ135) for financial support.

**Keywords:** asymmetric catalysis • bifunctional catalysis • heterogeneous catalyst • immobilization • mesoporous material

- [1] a) C. E. Song, *Handbook of Asymmetric Heterogeneous Catalysis* (Eds.: K. L. Ding, Y. Uozumi), Wiley-VCH, Weinheim, **2009**, pp. 25; b) P. J. Walsh, H. M. Li, C. A. de Parrodi, *Chem. Rev.* **2007**, *107*, 2503; c) M. Heitbaum, F. Glorius, I. Escher, *Angew. Chem.* **2006**, *118*, 4850; *Angew. Chem. Int. Ed.* **2006**, *45*, 4732; d) Z. Wang, G. Chen, K. L. Ding, *Chem. Rev.* **2009**, *109*, 322; e) M. Bartók, *Chem. Rev.* **2010**, *110*, 1663; f) A. Bartoszewicz, N. Ahlsten, B. Martín-Matute, *Chem. Eur. J.* **2013**, *19*, 7274.
- [2] a) C. Li, H. D. Zhang, D. M. Jiang, Q. H. Yang, *Chem. Commun.* **2007**, 547; b) H. Q. Yang, L. Zhang, L. Zhong, Q. H. Yang, C. Li, *Angew. Chem.* **2007**, *119*, 6985; *Angew. Chem. Int. Ed.* **2007**, *46*, 6861; c) S. Y. Bai, H. Q. Yang, P. Wang, J. S. Gao, B. Li, Q. H. Yang, C. Li, *Chem. Commun.* **2010**, *46*, 8145; d) Y. Shen, Q. Chen, L.-L. Lou, K. Yu, F. Ding, S. Liu, *Catal. Lett.* **2010**, *137*, 104.
- [3] a) J. M. Thomas, R. Raja, *Acc. Chem. Res.* **2008**, *41*, 708; b) M. D. Jones, R. Raja, J. M. Tothomas, B. F. G. Johnson, D. W. Lewis, J. Rouzaud, K. D. M. Harris, *Angew. Chem.* **2003**, *115*, 4462; *Angew. Chem. Int. Ed.* **2003**, *42*, 4326.
- [4] H. J. Zhang, Z. Y. Li, P. P. Xu, R. F. Wu, Z. Jiao, *Chem. Commun.* **2010**, *46*, 6783.
- [5] L. Zhang, Y. N. Guo, J. Peng, X. Liu, P. Yuan, Q. H. Yang, C. Li, *Chem. Commun.* **2011**, *47*, 4087.
- [6] a) S. Tang, R. H. Jin, H. S. Zhang, H. Yao, J. L. Zhuang, G. H. Liu, H. X. Li, *Chem. Commun.* **2012**, *48*, 6286; b) H. S. Zhang, R. H. Jin, H. Yao, S. Tang, J. L. Zhuang, G. H. Liu, H. X. Li, *Chem. Commun.* **2012**, *48*, 7874; c) W. Xiao, R. H. Jin, T. Y. Cheng, D. Q. Xia, H. Yao, F. Gao, B. X. Deng, G. H. Liu, *Chem. Commun.* **2012**, *48*, 11898; d) D. Q. Xia, T. Y. Cheng, W. Xiao, K. T. Liu, Z. L. Wang, G. H. Liu, H. L. Li, W. Wang, *ChemCatChem* **2013**, DOI: 10.1002/cctc.201200954; e) Y. Q. Sun, G. H. Liu, H. Y. Gu, T. Z. Huang, Y. L. Zhang, H. X. Li, *Chem. Commun.* **2011**, *47*, 2583; f) J. Long, G. H. Liu, T. Y. Cheng, H. Yao, Q. Q. Qian, J. L. Zhuang, F. Gao, H. X. Li, *J. Catal.* **2013**, *298*, 41.
- [7] a) O. Soltani, M. A. Ariger, H. Vázquez-Villa, E. M. Carreira, *Org. Lett.* **2010**, *12*, 2893; b) H. Vázquez-Villa, S. Reber, M. A. Ariger, E. M. Carreira, *Angew. Chem.* **2011**, *123*, 9141; *Angew. Chem. Int. Ed.* **2011**, *50*, 8979; c) R. ter Halle, E. Schulz, M. Lemaire, *Synlett* **1997**, 1257.
- [8] Y. L. Huang, S. Xu, V. S. Y. Lin, *Angew. Chem.* **2011**, *123*, 687; *Angew. Chem. Int. Ed.* **2011**, *50*, 661.
- [9] S. Hiraoka, M. Shiro, M. Shionoya, *J. Am. Chem. Soc.* **2004**, *126*, 1214.
- [10] S. Ogo, N. Makihara, Y. Watanabe, *Organometallics* **1999**, *18*, 5470.
- [11] V. Cauda, A. Schlossbauer, J. Kecht, A. Zürner, T. Bein, *J. Am. Chem. Soc.* **2009**, *131*, 11361.
- [12] P. F. W. Simon, R. Ulrich, H. W. Spiess, U. Wiesner, *Chem. Mater.* **2001**, *13*, 3464.
- [13] O. Kröcher, O. A. Köppel, M. Fröba, A. Baiker, *J. Catal.* **1998**, *178*, 284.
- [14] a) D. Moon, J. Lee, *Langmuir* **2012**, *28*, 12341; b) C. Wang, Y. Zhou, M. Y. Ge, X. B. Xu, Z. L. Zhang, J. Z. Jiang, *J. Am. Chem. Soc.* **2010**, *132*, 46.

Received: May 3, 2013

Published online on ■ ■ ■ ■, 0000